UAV-Assisted Spectrum Mapping System Based on Tensor Completion Scheme

Xiaofu Du[1,2], Qiuming Zhu[1,2(✉)], Qihui Wu[1,2], Weizhi Zhong[1,3], Yang Huang[1,2], Neng Cheng[1,2], and Dong Liu[1,2]

[1] Key Laboratory of Dynamic Cognitive System of Electromagnetic Spectrum Space, Ministry of Industry and Information Technology, Nanjing University of Aeronautics and Astronautics, Nanjing 210016, China
{duxiaofu,zhuqiuming,wuqihui,zhongwz, yang.huang.ceie,chengn1208}@nuaa.edu.cn, 1760523985@qq.com
[2] College of electronic and information engineering, Nanjing University of Aeronautics and Astronautics, Nanjing 211106, China
[3] College of Astronautics, Nanjing University of Aeronautics and Astronautics, Nanjing 210016, China

Abstract. Electromagnetic spectrum is an indispensable resource in the current Information Age. Along with the rapid development of integrated space and terrestrial communication networks, spectrum shortage is one of the challenges faced by electromagnetic spectrum resource utilization in both airspace and terrestrial space. In order to realize the effective supervision and allocation of spectrum resources, a UAV-assisted spectrum mapping system based on tensor completion scheme is proposed. By using a UAV platform, the hardware system can acquire the multi-dimensional spectrum information, i.e., the geographical location and spectrum power, quickly and flexibly in the 3D space. The high accuracy low rank tensor completion (HaLRTC) algorithm is adopted to process the multi-dimensional spectrum data, i.e., data completion and map construction. The output spectrum map can display the characteristics of electromagnetic spectrum space more intuitively, and provide a solid basis for dynamic spectrum management. Finally, the proposed spectrum map system is tested under campus scenario.

Keywords: Spectrum map · Spectrum visualization · Tensor completion · UAV

1 Introduction

Spectrum resource is a scarce resource, which is not only the core of wireless communication technology but also national strategy resource [1]. With the development and wide application of integrated space and terrestrial communication networks, spectrum resource is becoming scarcer and scarcer in both the terrestrial space and airspace. How to efficiently allocate and utilize the existing

M. Guan and Z. Na (Eds.): MLICOM 2020, LNICST 342, pp. 16–26, 2021.
https://doi.org/10.1007/978-3-030-66785-6_2

spectrum resource has always been an important and urgent issue. The first step of improving spectrum utilization is to cognize the current spectrum usage. However, it's difficult to cognize spectrum information from the electromagnetic environment directly or by traditional instruments. One solution is to obtain the spectrum map and display the spectrum usage of underlying region intuitively. Therefore, it is necessary and urgent to develop a spectrum mapping system that can collect and display the spectrum information in 3D space and then to improve the efficiency of spectrum utilization.

It should be mentioned that the spectrum map is also referred as radio environment map (REM) [2] and radio frequency maps [3], and the process of spectrum map construction is termed as spectrum cartography [4] or spectrum visualization. Actually, the spectrum map visually displays the spectrum information on a map and represents the distribution of different radio parameter over a geographical area, such as received signal strength, channel gain, and interference [5]. First of all, spectrum map construction needs spectrum measurements to collect original spectrum data, the mainstream method is to deploy ground spectrum sensors that can collect the spectrum data from their respective locations in the region of interest [6]. In [7], the authors builded a distributed spectrum monitoring network to collect data. In [1], the authors used spectrum detection nodes that can acquire and record received signal strength, the current GPS, temperature, humidity, and other parameters. In [8], the measurements were collected by multiple distributed radars or radio frequency sensors in the different locations. Note that the above methods can only acquire the 2D spectrum data, while the 3D spectrum map is needed for the integrated space and terrestrial communication networks.

Since the measured data are usually incomplete, spectrum completion based on measured data is necessary and crucial. In [8,10] and [11], the Kriging spatial interpolation was adopted to estimate the spectrum information of geographical locations without measurements. In [12] and [13], the authors adopted the LIvE method and SNR-aided method, respectively, which utilized transmitter parameters and radio propagation modeling. It has better performance for the spectrum map construction than the Kriging spatial interpolation. However, all aforementioned methods are only suitable to the 2D spectrum map construction. This paper aims to fill these gaps. The major contributions and novelties of this paper are summarized as follows:

1) We develop a UAV-assisted spectrum mapping system, which mainly consists of UAV platform, spectrum monitoring module, data transmission module, and spectrum data cognition terminal. The system can acquire the multi-dimensional spectrum information including geographical location information and spectrum power quickly and flexibly in 3D space.
2) By dividing the three-dimension measurement space into serval 3D grids, we model the collected multi-dimensional spectrum data used for 3D spectrum map construction as a three-order tensor which contains aerial spectrum information. Based on the tensor completion idea, the 3D spectrum map is constructed. To our best knowledge, the existing literature hardly studies on

constructing 3D spectrum map including multi-dimensional spectrum information.

The remainder of the paper is organized as follows. Section 2 presents the hardware system structure. Section 3 introduces the spectrum map construction based on the tensor completion scheme. The experiment and tested results are provided in Sect. 4. The conclusions are drawn in Sect. 5.

2 Hardware System

The system is mainly composed of four modules: UAV platform, spectrum monitoring module, data transmission module and spectrum data cognition terminal. Spectrum monitoring module and data transmission module are mounted on UAV platform. UAV platform, spectrum monitoring module and data transmission module constitute the aerial part of the system, while the spectrum data cognition terminal constitutes the ground part of the system. The UAV platform mainly includes the GPS receiving submodule, image capturing submodule and flight control submodule; the spectrum monitoring module mainly consists of a spectrum receiver and an omnidirectional antenna; data transmission module mainly consists of a microcomputer and an airborne data link terminal; the spectrum data cognition terminal is mainly comprised of core cognition submodule, ground data receiving submodule and remote-control submodule. The hardware system structure is shown in Fig. 1 detailedly.

The UAV platform can provide the strong mobility in airspace for the system [14]. The spectrum monitoring module can collect the spectrum information around the UAV in real time when the system runs. The data transmission module can transmit the collected spectrum information and the other information such as geographical location information to the spectrum data cognition terminal and receive the flight control information from the spectrum data cognition terminal, which uses beamforming technology [15,16] and multiple-input multiple-output (MIMO) technology [17,18]. The spectrum data cognition terminal can use tensor completion algorithm to process the collected multi-dimensional spectrum data, thereby realizing 3D spectrum map construction of the measurement region. Some system performance parameters are shown in Table 1.

Table 1. System parameters.

Parameter	Value
Spectrum range	9 kHz to 8 GHz
Frequency resolution	1 Hz
Sensitivity	−155 dBm
The type of antenna	Omnidirectional
UAV's velocity	26 m/s (horizontal); 8 m/s (vertical)

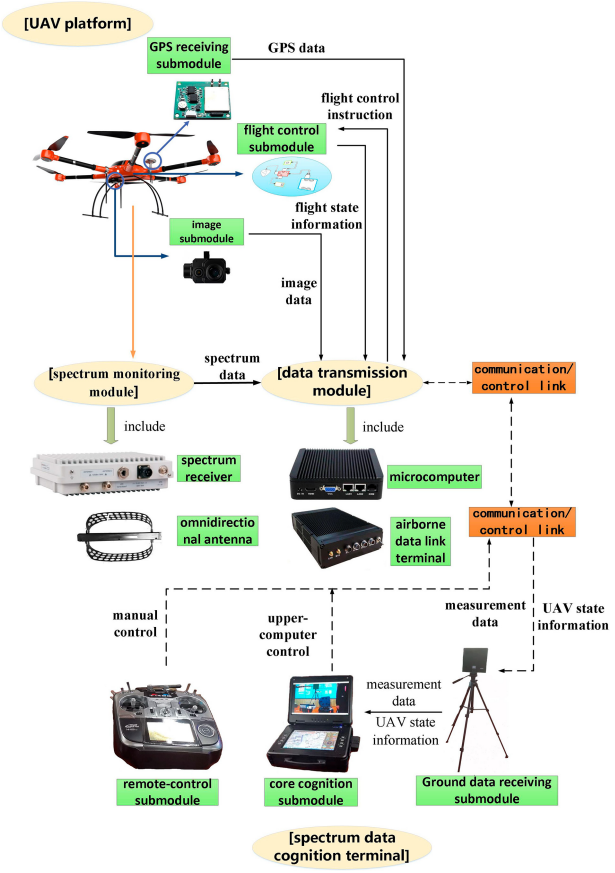

Fig. 1. Hardware structure of proposed system.

3 Spectrum Data Processing

3.1 Data Model of Spectrum Map

An n-order spectrum tensor can be defined as $\chi \in R^{I_1 \times I_2 \times \ldots \times I_n}$, and $x_{i_1,i_2,\ldots,i_n}$ denotes the n-th element of the tensor χ. As shown in Fig. 2, the real-world spectrum data that the system collects in stereoscopic space can be modeled as a three-order tensor $\chi \in R^{I_1 \times I_2 \times I_3}$. The x-axis, y-axis and z-axis corresponds to the coordinates x, y and z of the 3D stereoscopic space. Each element x_{i_1,i_2,i_3} in this spectrum tensor denotes the received signal strength in the position of the abscissa i_1, the position of the ordinate i_2 and the position of vertical coordinate i_3. In Fig. 2, different colors are used in denoting different received signal strength. Note that, the display form of three-order tensor in Fig. 2 can also be viewed as a 3D spectrum map, and what the spectrum map that our system constructs displays is the 3D spatial distribution of received signal strength in a particular area.

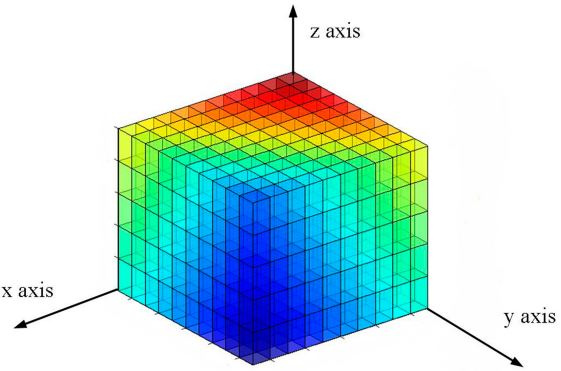

Fig. 2. Model for spectrum map data.

In practical applications, owing to these factors such as the terrain environment, the number of spectrum monitoring nodes (i.e. spectrum sensors), deployment locations, and measurement equipment performance have certain limitations, which makes the electromagnetic environment observation or spectrum measurements can only be incomplete and limited [5]. In other words, it is impractical to have measurements at each location in the measurement area. Moreover, when the spectrum tensor acquires a large amount of measurements for high accuracy of constructed spectrum map, the overhead of time or material resource will be narrowed down by sampling. Therefore, retrieving the incomplete spectrum data based on the limited measurements is essential for 3D spectrum map construction.

3.2 Spectrum Map Construction

Given a subset Ω, data in the subset Ω indicate the elements corresponding to real measurement data in χ, the other elements corresponding to unknown spectrum data of these locations without measurements would set to be "0". The subset tensor χ_Ω can be defined as:

$$\chi_\Omega = \begin{cases} \chi, (i_1, i_2, ..., i_n) \in \Omega \\ 0, \text{otherwise} \end{cases} \tag{1}$$

Because of the low-rank property of the real-world spectrum tensor [19], the spectrum tensor completion for the values of "unknown" elements in χ can be modeled as an optimization problem, which uses the known subset to complete the tensor data, specifically implemented as the following problem:

$$\begin{aligned} &\min \|\chi\|_* \\ &s.t. \chi_\Omega = \Gamma_\Omega \end{aligned} \tag{2}$$

where $\|\cdot\|_*$ originally denotes the tightest convex envelop for the rank of matrices, and it extends to the tensor in this case, χ_Ω, Γ_Ω are n-mode spectrum tensors

with the same size in each mode, entries of Γ from the set Ω are given by real measurement data while the remaining entries are missing and χ is the incomplete spectrum tensor to be completed. For low rank tensor completion problem, computing the rank of a tensor (mode number > 2) is an NP hard problem [20]. So, the following definition for the tensor trace norm is introduced [19],

$$\|\chi\|_* := \sum_{i=1}^{n} \alpha_i \left\|\chi_{(i)}\right\|_* \tag{3}$$

where $\chi_{(i)} \in R^{I_i \times (I_1 \times \ldots \times I_{i-1} \times I_{i+1} \times \ldots \times I_n)}$ denotes the matrix unfolded by tensor χ in the i-th mode, $\alpha_i > 0$ and $\sum_{i=1}^{n} \alpha_i = 1$, $\left\|\chi_{(i)}\right\|_*$ denotes the norm of the unfolded matrix $\chi_{(i)}$. The trace norm of a tensor is consistent with all the matrices unfolded along each mode. Under this definition, the optimization problem can be converted to the following formula,

$$\begin{aligned} &\min_{\chi} \sum_{i=1}^{n} \alpha_i \left\|\chi_{(i)}\right\|_* \\ &s.t. \chi_\Omega = \Gamma_\Omega \end{aligned} \tag{4}$$

We adopt an efficient algorithm proposed in [21] to deal with this tensor completion problem in (4). The algorithm can work even with a small amount of samples and estimate larger missing regions of the spectrum data. Although its convergence rate is not the fastest, the convergence of the algorithm is guaranteed.

The problem in (4) is difficult to tackle due to the interdependence among the matrix trace norm terms. In order to simplify the problem in (4), additional tensors $\varphi_1, ..., \varphi_n$ are introduced [19]. Therefore, the following equivalent formulation can be obtained:

$$\begin{aligned} &\min_{\chi, \varphi_i} \sum_{i=1}^{n} \alpha_i \left\|\varphi_{i(i)}\right\|_* \\ &s.t. \chi = \varphi_i \quad for\, i = 1, ..., n \\ &\chi_\Omega = \Gamma_\Omega \end{aligned} \tag{5}$$

The augmented Lagrangian function is defined as follows accordingly:

$$\begin{aligned} &L_\rho(\chi, \varphi_1, ..., \varphi_n, \gamma_1, ..., \gamma_n) \\ &= \sum_{i=1}^{n} \alpha_i \left\|\varphi_{i(i)}\right\|_* + \langle \chi - \varphi_i, \gamma_i \rangle + \frac{\rho}{2} \|\varphi_i - \chi\|_F^2 \end{aligned} \tag{6}$$

where $\langle \chi, \gamma \rangle$ is the inner product of tensor χ and tensor γ, they are two n-mode tensors with the same size in each mode, it can be also endowed with $\langle \chi, \gamma \rangle = \sum_{i_1} \sum_{i_2} \ldots \sum_{i_n} x_{i_1, \ldots, i_n} y_{i_1, \ldots, i_n}$; $\|\cdot\|_F$ is the Frobenius norm; ρ is the penalty parameter of the penalty function; γ_i is Lagrangian multiplier.

According to the framework of ADMM applied by the algorithm, the augmented Lagrangian function is applied to update φ_i, χ_i and γ_i iteratively.

$$\begin{aligned}&\left\{\varphi_1^{k+1}, ..., \varphi_n^{k+1}\right\}\\&= \arg\min_{\varphi_1,...,\varphi_n} L_\rho(\chi^k, \varphi_1, ..., \varphi_n, \gamma_1^k, ...\gamma_n^k)\end{aligned} \tag{7}$$

$$\chi^{k+1} = \arg\min_{\chi \in Q} L_\rho(\chi, \varphi_1^{k+1}, ..., \varphi_n^{k+1}, \gamma_1^k, ..., \gamma_n^k) \tag{8}$$

$$\gamma_i^{k+1} = \gamma_i^k - \rho(\varphi_i^{k+1} - \chi^{k+1}) \tag{9}$$

where $Q = \left\{\chi \in R^{I_1 \times I_2 \times ... \times I_n} | \chi_\Omega = \Gamma_\Omega\right\}$ in (8), and superscript k represents the k-th iteration.

This specific algorithm is summarized in **Algorithm 1**, where $fold_i\left[\chi_{(i)}\right]$ denotes the operation of folding the matrix $\chi_{(i)}$ to the tensor χ in i-th mode; $D_\tau(\mathbf{X})$ represents the "shrinkage" operator of the matrix $\mathbf{X}$, which is defined as

$$D_\tau(\mathbf{X}) = \mathbf{U}\Sigma_\tau\mathbf{V}^{\mathrm{T}} \tag{10}$$

where $\mathbf{U}$ and $\mathbf{V}$ are the unitary matrices in the singular value decomposition $\mathbf{X} = \mathbf{U}\sum\mathbf{V}^{\mathrm{T}}$ for $\mathbf{X}$, and $\sum_\tau = diag(\max(\sigma_i - \tau, 0))$, σ's are the singular values.

4 Measurements Under Campus Scenario

4.1 Experiment Setup

The measurement campaigns were carried out in Jiangning campus of Nanjing University of Aeronautics and Astronautics. As shown in Fig. 3(a), the measurement region is divided into 20 × 20 grids. In order to acquire the real-world multi-dimensional spectrum data containing aerial spectrum data, we operated the aerial part of the system to fly randomly in the measurement region and measure the received signal strength in 20 m, 25 m and 30 m high above the

Algorithm 1. HaLRTC: High Accuracy Low Rank Tensor Completion

Input: The number of iterations K, χ with $\chi_\Omega = \Gamma_\Omega$ and ρ.
Output: The completed spectrum data used for spectrum map construction χ.

1: Set $\chi_\Omega = \Gamma_\Omega$, $\chi_{\bar{\Omega}} = 0$, $\gamma_i = 0$ and $\varphi_i = 0$ $(i = 1, ..., n)$.
2: **for** $k = 0$ to K **do**
3: **for** $i = 1$ to n **do**
4: $\varphi_i = fold_i\left[D_{\frac{\alpha_i}{\rho}}\left(\chi_i + \frac{1}{\rho}\gamma_{i(i)}\right)\right]$.
5: **end for**
6: $\chi_\Omega = \frac{1}{n}\left(\sum_{i=1}^{n}\left(\varphi_i - \frac{1}{\rho}\gamma_i\right)\right)_{\bar{\Omega}}$;
7: $\gamma_i = \gamma_i - \rho(\varphi_i - \chi)$.
8: **end for**

ground respectively. The frequency band between 470 MHz and 700 MHz was chosen as the observation frequency band. For simplicity, it is assumed that the received signal strength of each grid is almost consistent during the experiment. Hence, the real-world measurement data used for spectrum map construction in the experiment can be modeled as a tensor whose size is $20 \times 20 \times 3$ by corresponding the measurement locations to the divided grids. The proposed spectrum mapping system used for measurement is shown in Fig. 3(b).

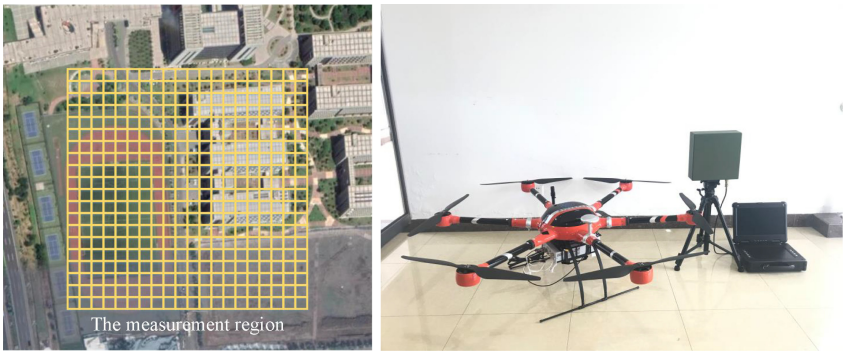

(a) (b)

Fig. 3. (a) The measurement region under campus scenario; (b) The proposed spectrum mapping system.

4.2 Measured Results

After the real-world measured spectrum data (see Fig. 4(a)) is complemented by the adopted tensor completion algorithm, the 3D spectrum map of the measurement region is constructed (see Fig. 4(b)), where different colors denote different received signal strength. The darker the color, the lower received signal strength of the location marked with the color in the observation frequency band. The divisiory $20 \times 20 \times 3$ 3D grids in our spectrum map are the equal of the pixels of 2D spectrum map. Through the constructed spectrum map, the situation of 3D spectrum usage in the measurement region is displayed intuitively.

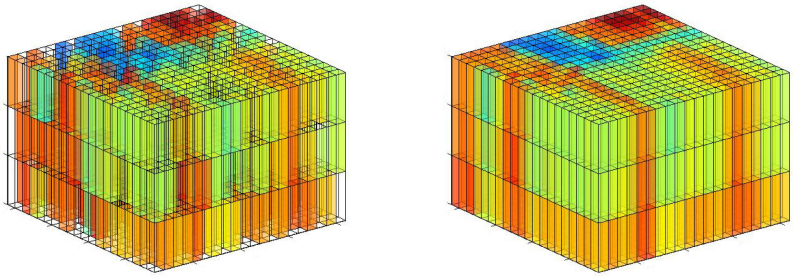

(a) (b)

Fig. 4. The real-world measured spectrum data (a) before completion, (b) after completion.

5 Conclusions

The UAV-assisted spectrum mapping system based on tensor completion scheme has been developed in this paper. The system can collect the multi-dimensional spectrum information quickly and intelligently in 3D space. The tensor completion algorithm HaLRTC has been adopted in the multi-dimensional spectrum data completion to construct the 3D spectrum map. Thus, the invisible spectrum space can be visualized to intuitively show the usage of regional spectrum, which is convenient for discovering spectrum holes and managing spectrum dynamically. The spectrum map construction effectiveness of the system has been verified under campus scenario. For the future work, we would take the frequency and time information into the collected spectrum data and obtain the spectrum map including more information.

Acknowledgements. This work was supported in part by the National Key Scientific Instrument and Equipment Development Project under Grant No. 61827801, in part by Aeronautical Science Foundation of China No. 201901052001, and in part by the Fundamental Research Funds for the Central Universities No. NS2020026 and No. NS2020063.

References

1. Guo, X., Zhang, Y., Chen, Z., He, C., Hai, W.: Distributed electromagnetic spectrum detection system based on self-organizing network. In: 2018 12th International Symposium on Antennas, Propagation and EM Theory (ISAPE), Hangzhou, China, pp. 1–5 (2018)
2. Pesko, M., Javornik, T., et al.: Radio environment maps: the survey of construction methods. KSII Trans. Internet Inf. Syst. **81**(3), 3789–3809 (2014)

3. Vanhoy, G., Volos, H., Bastidas, C.E.C., Bose, T.: a spatial interpolation method for radio frequency maps based on the discrete cosine transform. In: MILCOM 2013–2013 IEEE Military Communications Conference, San Diego, CA, pp. 1045–1050 (2013)
4. Jayawickrama, B.A., Dutkiewicz, E., Oppermann, I., Fang, G., Ding, J.: Improved performance of spectrum cartography based on compressive sensing in cognitive radio networks. In: 2013 IEEE International Conference on Communications (ICC), Budapest, pp. 5657–5661 (2013)
5. Lu, J., Zha, S., Huang, J., Liu, P., Chen, G., Xu, S.: The iterative completion method of the spectrum map based on the difference of measurement values. In: 2018 IEEE 3rd International Conference on Signal and Image Processing (ICSIP), Shenzhen, pp. 255–259 (2018)
6. Zha, S., Huang, J., Qin, Y., Zhang, Z.: An novel non-parametric algorithm for spectrum map construction. In: 2018 International Symposium on Electromagnetic Compatibility (EMC EUROPE), Amsterdam, pp. 941–944 (2018)
7. Patino, M., Vega, F.: Model for measurement of radio environment maps and location of white spaces for cognitive radio deployment. In: 2018 IEEE-APS Topical Conference on Antennas and Propagation in Wireless Communications (APWC), Cartagena des Indias, pp. 913–915 (2018)
8. Melvasalo, M., Koivunen, V., Lundn, J.: Spectrum maps for cognition and coexistence of communication and radar systems. In: 2016 50th Asilomar Conference on Signals, Systems and Computers, Pacific Grove, CA, pp. 58–63 (2016)
9. Chaudhari, S., et al.: Spatial interpolation of cyclostationary test statistics in cognitive radio networks: methods and field measurements. IEEE Trans. Veh. Technol. **67**(2), 1113–1129 (2018)
10. Janakaraj, P., Wang, P., Chen, Z.: Towards cloud-based crowd-augmented spectrum mapping for dynamic spectrum access. In: 2016 25th International Conference on Computer Communication and Networks (ICCCN), Waikoloa, HI, pp. 1–7 (2016)
11. Mao, D., Shao, W., Qian, Z., Xue, H., Lu, X., Wu, H.: Constructing accurate radio environment maps with kriging interpolation in cognitive radio networks. In: 2018 Cross Strait Quad-Regional Radio Science and Wireless Technology Conference (CSQRWC), Xuzhou, pp. 1–3 (2018)
12. Yilmaz, H.B., Tugcu, T.: Location estimation-based radio environment map construction in fading channels. Wireless Commun. Mobile Comput. **15**(3), 561–570 (2015)
13. Sun, G., van de Beek, J.: Simple distributed interference source localization for radio environment mapping. In: 2010 IFIP Wireless Days, Venice, pp. 1–5 (2010)
14. Cui, Z., Briso-Rodrguez, C., Guan, K., Calvo-Ramrez, C., Ai, B., Zhong, Z.: Measurement-based modeling and analysis of UAV air-ground channels at 1 and 4 GHz. IEEE Antennas Wirel. Propag. Lett. **18**(9), 1804–1808 (2019)
15. Zhong, W., Xu, L., Zhu, Q., Chen, X., Zhou, J.: MmWave beamforming for UAV communications with unstable beam pointing. China Commun. **16**(1), 37–46 (2019)
16. Zhong, W., Xu, L., Liu, X., Zhu, Q., Zhou, J.: Adaptive beam design for UAV network with uniform plane array. Phys. Commun. **34**, 58–65 (2019)
17. Zhu, Q., Wang, Y., Jiang, K., Chen, X., Zhong, W., Ahmed, N.: 3D non-stationary geometry-based multi-input multi-output channel model for UAV-ground communication systems. IET Microwaves Antennas Propag. **13**(8), 1104–1112 (2019)

18. Zhu, Q., Jiang, K., Chen, X., Zhong, W., Yang, Y.: A novel 3D non-stationary UAV-MIMO channel model and its statistical properties. China Commun. **15**(12), 147–158 (2018)
19. Tang, M., Ding, G., Xue, Z., Zhang, J., Zhou, H.: Multi-dimensional spectrum map construction: a tensor perspective. In: 2016 8th International Conference on Wireless Communications & Signal Processing (WCSP), Yangzhou, pp. 1–5 (2016)
20. Hillar, C.J., Heng Lim, L.: Most tensor problems are NP hard. Computing Research Repository. http://arxiv.org/abs/0911.1393 (2009)
21. Liu, J., Musialski, P., Wonka, P., Ye, J.: Tensor completion for estimating missing values in visual data. IEEE Trans. Pattern Anal. Mach. Intell. **35**(1), 208–220 (2013)